Vol. **128** (2015) *ACTA PHYSICA POLONICA A* No. 5

Proc. of the X Int. Conf. — Ion Implantation and other Applications of Ions and Electrons, Kazimierz Dolny 2014

The Corrosion Enhancement due to Plasma Post-Oxidation Subsequent to Plasma Nitriding of a Steel AISI 4140

A.E. Muñoz-Castro[a,*], A. de la Piedad-Beneitez[b], R. Valencia-Alvarado[a],
R. López-Callejas[a,b], A. Mercado-Cabrera[a], R. Peña-Eguiluz[a]
and B.G. Rodriguez-Mendez[a]

[a]Instituto Nacional de Investigaciones Nucleares, Plasma Physics Laboratory,
AP 18-1027, CP 11801, Mexico D.F., Mexico
[b]Instituto Tecnológico de Toluca, Av. Tecnológico S/N, AP 890, Toluca, Mexico

The corrosion enhancement due to plasma post-oxidation subsequent to plasma nitriding of the samples of low alloy annealed steel AISI 4140 was evaluated. The plasma nitriding was carried out at ≈570 °C for 1–3 h in an atmosphere of 75% H_2 and 25% N_2. After this process post-oxidation at ≈450 °C in a gas mixture, air and dry air-like was conducted for an hour. The treated samples were characterized using the XRD, SEM, AFM, potentiodynamic polarization and Vickers microhardness tests. The outcome of combined processes showed the presence of ε and γ' nitrided phases in the inner compound layer and in the outer one mostly of magnetite phase and barely visible of hematite one without using H_2 in the post-oxidation process. Also in these processes, the corrosion potential proved to be lower in the treated specimens than the untreated ones, and the corrosion current decreased up to one order of magnitude when treated in environment air and air-like ambient.

DOI: 10.12693/APhysPolA.128.824

PACS: 52.77.–j, 52.40.Hf, 81.40.–z, 81.65.–b, 81.65.Mq

1. Introduction

It is unanimously recognized in the literature that the aim of post-oxidation is to have a Fe_3O_4 (magnetite) layer avoiding α-Fe_2O_3 (hematite) on the ferrous alloy surfaces subsequent to plasma nitriding in order to enhance the tribological properties and corrosion resistance [1] whereas the iron nitriding increases the wear resistance. The latter can be achieved through the formation of an inner compound layer consisting of ε-$Fe_{2-3}N$, γ'-Fe_4N and other nitrides [2]; the former through an outer layer which should essentially contain magnetite, a very low content of hematite and probably FeO as well. The hematite phase layer is porous, brittle and a little adherent [3] while the magnetite one denser and more homogeneous so with a higher corrosion performance and a lower friction coefficient [4].

Nowadays the interest in post-oxidation in low alloy steels has grown including plain steels [5, 6]. The applications of this duplex process are to improve the surface properties of pump components, spring washers under corrosive and tribological loads [7] and to provide a high-performance mechanical system for hydraulic and automotive parts [3, 8]. Attempts were made to conduct on post-oxidation processes with different atmospheres: O_2, H_2O and CO_2 with or without H_2 or Ar in order to obtain magnetite resulting in the presence of hematite [6, 8, 9]. This paper is focused on investigating the anticorrosive effect of plasma post-oxidation in the two types of atmospheres: dry air-like (dal) and environmental air (air) without using H_2 after plasma nitriding on low alloy AISI 4140 steel.

2. Experimental

Annealed low alloy AISI 4140 steel of the following chemical composition (in wt%): 0.40 C, 0.90 Mn, 0.03 P, 0.03 S, 0.25 Si, 0.95 Cr, 0.20 Mo and Fe balance. The samples used in this study were discs of 9 mm diameter and 3 mm thick cut off a rod of 12.7 mm diameter. The samples were machined, polished using SiC grits from 600 to 2000 and ultrasonically cleaned in acetone before being placed into the reactor.

The ion nitriding on the samples was achieved by a RF inductive discharge in 75% H_2 and 25% N_2 atmosphere at 6 Pa working pressure after been evacuated down to a 5×10^{-2} Pa base pressure. Before their treatment, the samples were finally cleansed by a twenty-minute bombardment with Ar ions. The samples were nitrided for one (1hN), two (2hN) and three (3hN) hours at ≈570 °C [10]. Post-oxidation was performed for one hour (1hPO) at ≈450 °C, in the two types of atmosphere: in extra dry air-like (dal) and in environmental air (air).

The compound and oxidized layers were observed and the depths measured by scanning electron microscopy (SEM). For this purpose the samples were previously cross-sectionally cut, metallographically prepared and etched with a 2.5% Nital solution. In order to follow up the microstructure evolution, a scanning electron microscope was used while the energy dispersive spectroscopy (EDS) technique was applied in order to evaluate the nitrogen and oxygen contents. X-ray diffraction of Cu K_α

---

[*] corresponding author; e-mail: arturo.munoz@inin.gob.mx

radiation (1.5405 Å) determined the phases. The filler effect of post-oxidation was evidenced by the atomic force microscopy (AFM) micrographs. The surface microhardness was assessed with a Vickers tester using a 500 g load by averaging every six measurements. Potentiodynamic tests in 3.5% NaCl solution were applied at room temperature with the potentials ranging from -800 to 1200 mV (with respect to a saturated calomel electrode) at a scan rate of 1 mV/s so as to determine the corrosion performance.

3. Results and discussion

In order to investigate the surface morphology and elemental content, the SEM and EDS analyses were made. The SEM micrograph in Fig. 1 shows the oxidized surface topography of a typical sample before being nitrided. There are three types of zones: white and black, white, and black; the EDS analyses show iron oxides and carbon formation. The zone mostly representative is that of the arrow pointing to the EDS spectrum with no carbon content, therefore, there is no significant presence of re-deposition. The EDS analyses in at.% of oxygen, iron and nitrogen, as well as the corresponding O/Fe and O/N ratio in the surface layer are listed in Table I, 1hN+1hPO means a one hour nitriding and an hour post-oxidation. The O/Fe ratio indicates estimation of oxygen content which could be attributed to the formation of small amounts of $Fe(OH)_2$, $Fe(OH)_3$, etc. The sample treated at 2hN+1hPO with environmental air at both O/Fe and O/N ratios is the lowest compared to other samples treated which indicates formation of magnetite phase.

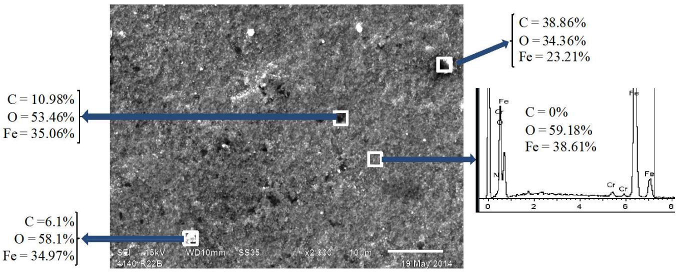

Fig. 1. Topographic view of the oxidized layer of a typical sample.

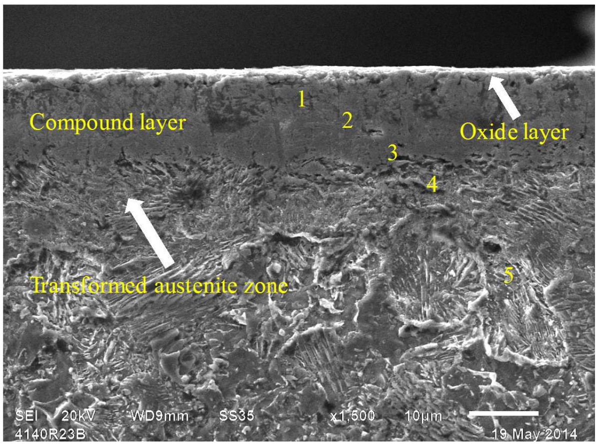

Fig. 2. Cross-view of the compound and oxidized layers of a typical sample.

TABLE I

Atomic percentage of the oxidized layer by EDS.

	Dry air						Environmental air					
	1hN+1hPO		2hN+1hPO		3hN+1hPO		1hN+1hPO		2hN+1hPO		3hN+1hPO	
Ratios	%O=60.35		%O=59.38		%O=60.4		%O=55.69		%O=54.36		%O=59.18	
	%Fe	%N	%Fe	%N	%Fe	%N	%Fe	%N	%Fe	%N	%Fe	%N
	32.29	0.96	31.47	3.91	37.54	1.02	37.05	4.28	37.25	5.16	38.61	3.76
O/Fe	1.87		1.88		1.61		1.50		1.45		1.53	
O/N	62.86		15.18		59.21		13.01		10.53		15.73	

The SEM micrograph in Fig. 2 depicts the compound nitrided layer, oxidized layer, and transformed austenite zone, observed in differently treated samples. This reflects the compound and oxidized layers stability due to this type of treatment. The EDS technique associated with SEM was used in order to evaluate the nitrogen content from the EDS spectra in the zones: (1) 23.4 at.%, (2) 27.8 at.%, (3) 18.3 at.%, (4) 15.29 at.% and (5) 0 at.%. It means that in the central part of compound layer there is a maximum, decreasing toward the inner and outer zones as previously evaluated for the other samples which were only nitrided [10].

Figure 3 displays the AFM image of the sample before and after of oxidation treatment. It can be seen that the filler effect on the oxidized specimen (Fig. 3c, e, g) is evident in comparison with the nitrided samples (Figs. 3b, d, f). Comparing the untreated samples with nitrided and nitrided and post-oxidized ones, improvement in the smoothing of the latter can be observed. On the other hand, in the only nitrided samples, there is no difference in their morphology evidencing a low etching effect due to very low bias voltage on the samples.

XRD patterns of the untreated (Fig. 4a), nitrided (Fig. 4b) and nitrided post-oxidized (Fig. 4c–h) samples are shown in Fig. 4. The surface layer of the nitrided sample consists mainly of γ'-Fe4N and ε-$Fe_{2-3}N$ phases with a small diffraction peak of α-Fe phase. After

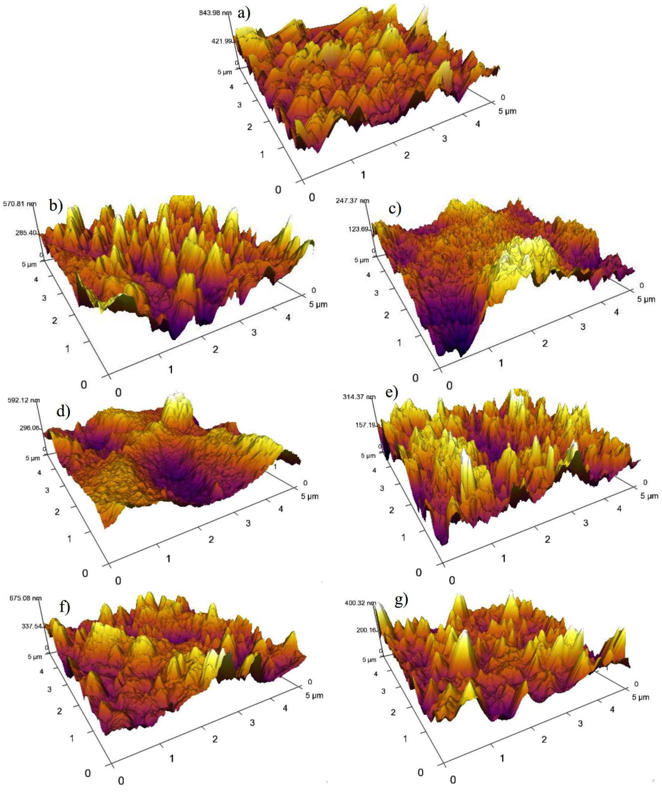

Fig. 3. Morphology of surface by AFM.

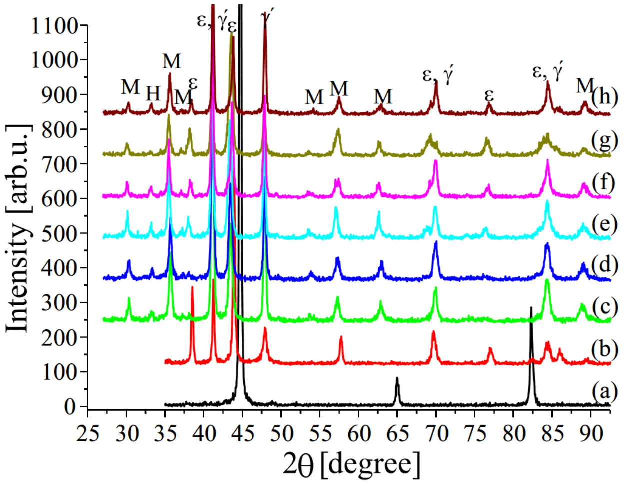

Fig. 4. Diffractogram corresponding to: (a) AISI 4140 untreated, (b) nitrided sample, (c) 1hN + 1hPO$_{\mathrm{dal}}$, (d) 2hN + 1hPO$_{\mathrm{dal}}$, (e) 3hN + 1hPO$_{\mathrm{dal}}$, (f) 1hN + 1hPO$_{\mathrm{air}}$, (g) 2hN + 1hPO$_{\mathrm{air}}$, (h) 3hN + 1hPO$_{\mathrm{air}}$. These graphs show the following phases: ε-Fe$_{2-3}$N, γ'-Fe$_4$N, magnetite (M = Fe$_3$O$_4$) and hematite (H = Fe$_2$O$_3$).

the post-oxidation process, formation of magnetite phase in all treated samples is evident. Particularly, for the post-oxidized samples with dry-air the hematite phase at $2\theta \approx 33.1°$ is also present; this is shown in Fig. 4c–e. When the post-oxidation process is carried out with environmental air (Fig. 4f–h) and without using H$_2$, this hematite peak decreases to be almost extinguished as shown in Fig. 4g, in a condition in which the sample was nitrided for 2 h. To explain the in-depth oxidized magnetite layer, it is suggested that hydrogenous species from the plasma, e.g. OH [11] are electrons carriers which due to their migration capability through grain boundaries, cracks and pores could reach deeper layers, releasing H to avoid formation of hematite via the intermediate reaction Fe:OH [12]; we believe that the OH species stem from the humidity of environmental air. Moreover, we think that nitrogen also plays a catalytic role in the magnetite formation at least if the percentage of nitrogen (≈80%) in the oxygen and nitrogen mixture is taken into account.

In general, the potentiodynamic tests displayed in Fig. 5 present a shift to higher potential (E_{corr}) values and lower corrosion currents (i_{corr}) when it compares the post-oxidized specimens with the untreated and only nitrided ones (see Table II). (i_{corr}) was calculated by the Tafel slopes with a software incorporated to the PC. It should be noted that the better electrochemical performance obtained for the samples post-oxidized in only environmental air (Fig. 5d–e) being the best (Fig. 5e) due to the lowest (i_{corr}) which is consistent with the low content of above mentioned hematite. Nevertheless for the sample treated for 3 h of nitriding and 1 h of post-oxidizing in dry air-like (sample c, Table II and Fig. 5, label c) a poor corrosion performance is observed.

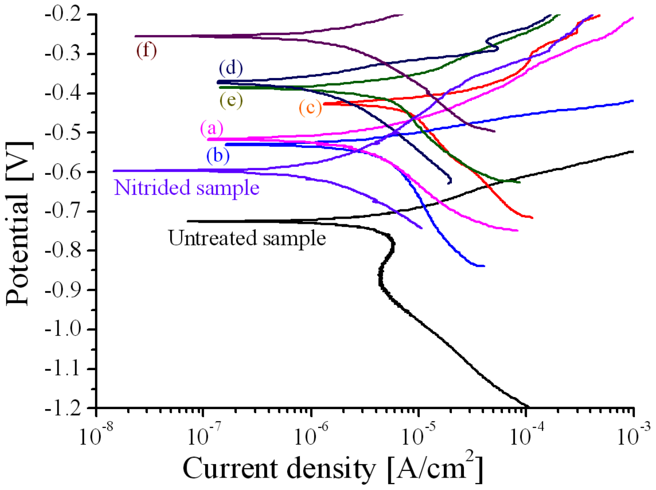

Fig. 5. Potentiodynamic tests of AISI 4140 untreated, nitrided sample, (a) 1hN + 1hPO$_{\mathrm{dal}}$, (b) 2hN + 1hPO$_{\mathrm{dal}}$, (c) 3hN + 1hPO$_{\mathrm{dal}}$, (d) 1hN + 1hPO$_{\mathrm{air}}$, (e) 2hN + 1hPO$_{\mathrm{air}}$, (f) 3hN + 1hPO$_{\mathrm{air}}$.

The surface hardness of all nitrided and post-oxidized pieces in dry air-like is on the average 740 HV while with atmospheric air 755 HV (see Table II), in both cases the microhardness is close to the only nitrided one, which means that microhardness is not compromised due to the presence of oxidized layer. The Vickers microhardness of the post-oxidized samples was less than the nitrided sample but was higher compared to the untreated one.

TABLE II

Potentiodynamic test and microhardness results.

Sample (Fig. 5)	Conditions	E_{corr} [mV]	i_{corr} [A/cm^2]	Microhardness [HV$_{500g}$]	relative to untreated and nitrided samples
untreated	–	–725	2.48×10^{-6}	269	1
nitrided	3h	–595	5.02×10^{-7}	818	3.04
a)	1hN+1hPO$_{\text{dal}}$	–515	3.37×10^{-7}	663	2.46/0.81
b)	2hN+1hPO$_{\text{dal}}$	–530	1.69×10^{-7}	759	2.82/0.93
c)	3hN+1hPO$_{\text{dal}}$	–424	4.24×10^{-6}	798	2.96/0.98
d)	1hN+1hPO$_{\text{air}}$	–371	2.97×10^{-7}	763	2.84/0.93
e)	2hN+1hPO$_{\text{air}}$	–385	1.42×10^{-7}	734	2.73/0.90
f)	3hN+1hPO$_{\text{air}}$	–255	5.32×10^{-7}	768	2.85/0.94

4. Conclusions

RF inductive plasma discharge nitriding is a useful tool to nitride and post-oxidize low alloy steels. The post-oxidation in both air and dry air-like ambient shows good corrosion performance after 2 h of nitriding process and 1 h of post-oxidation. With the post-oxidation in air, it is possible to obtain low content of hematite phase without using H_2 or other gases, particularly with 2 h of nitriding. The microhardness is close to the value of nitrided samples after the post-oxidation process. Post-oxidation in atmospheric air seems to be an attractive method in operation of the process and from an economical point of view.

Acknowledgments

This project has been partially funded by CONACyT, Mexico. The authors are grateful to Carlos Salinas for the technical support in SEM diagnostics, Isidoro Martínez in XRD, Julio César Zenteno in corrosion tests and Pavel López in AFM. The technical assistance by Pedro Ángeles Espinoza, María Teresa Torres M. and Isaías Contreras Villa is much appreciated.

References

[1] A. Esfahani, H.H. Sohi, J. Rassizadehghani, F. Mahboubi, 10.1016/j.vacuum.2007.05.005 *Vacuum* **82**, 346 (2008).

[2] Y. Li, L. Wang, D. Zhang, L. Shen, *Appl. Surf. Sci.* **256**, 4149 (2010).

[3] F. Mahboubi, M. Fattah, *Vacuum* **79**, 1 (2005).

[4] M. Zlatanović, N. Popović, Ž. Bogdanov, S. Zlatanović, *Surf. Coat. Technol.* **177**, 277 (2004).

[5] A.C. Rovani, R.R. Fischer, F. Cemin, F.G. Echeverrigaray, R.L.O. Basso, C.L.G. Amorim, G.V. Soares, I.J.R. Baumvol, C.A. Figueroa, *Scr. Mater.* **62**, 863 (2010).

[6] N. Karimzadeh, E.G. Moghaddam, M. Mirjani, K. Raeissi, *Appl. Surf. Sci.* **283**, 584 (2013).

[7] M. Mirjani, J. Mazrooei, N. Karimzadeh, F. Ashrafizadeh, *Surf. Coat. Technol.* **206**, 4389 (2012).

[8] J.M. Hong, Y.R. Cho, D.J. Kim, J.M. Baek, K.H. Lee, *Surf. Coat. Technol.* **131**, 548 (2000).

[9] A. Alsaran, H. Altun, M. Karakan, A. Çelik, *Surf. Coat. Technol.* **176**, 344 (2004).

[10] A. de la Piedad-Beneitez, A.E. Muñoz-Castro, R. Valencia-Alvarado, R. López-Callejas, A. Mercado-Cabrera, R. Peña-Eguiluz, B. Rodríguez-Méndez, S.R. Barocio, *Acta Phys. Pol. A* **123**, 904 (2013).

[11] L. Magne, S. Pasquiers, K. Gadonna, P. Jeanney, N. Blin-Simiand, F. Jorand, C. Postel, *J. Phys. D Appl. Phys.* **42**, 165203 (2009).

[12] C. Luvison, V. Sonda, A.C. Rovani, F. Cemin, F.G. Echeverrigaray, C. Aguzzoli, A.E. Crespi, C.L.G. Amorim, M.E.H. Maia da Costa, I.J.R. Baumvol, C.A. Figueroa, *Vacuum* **86**, 1268 (2012).